An Analytical Model for a Transient Vapor Plume on the Moon

Sanford S Davis

Space Science Division, NASA Ames Research Center, Moffett Field CA 94035

Naturally occurring transient events were observed for many centuries on the Moon and nearby asteroids. Artificially induced impacts on near-Earth bodies are now being used to study a wide range of geomorphic phenomena. In this paper an analytical theory is used to predict the flash event that signals the initial phase of a surface impact. The model predicts the wave form, duration, and energy content of the vapor plume starting only with the kinetic energy of the impactor. The theory is applied to the planned early 2009 LCROSS lunar impact where the impact flash event is predicted. The transient radiation emitted by the impact can be used to obtain some relevant parameters and is predicted to be energetic enough to be captured by 1- to 5-m class terrestrial telescopes.

Introduction

The Moon is subject to a variety of naturally occurring transient events. Hughes 1980 reports “glows, hazes, mists, brief color changes, and obscurations of lunar surface features” recorded by centuries of observations. A catalogue of transient lunar phenomena over more than three hundred years was compiled by Cameron 1972, 1975. These events are attributed to a number of sources ranging from out gassing and impact events to electrostatic repulsion of lunar dust. The Leonid meteor shower of 1999 was an excellent opportunity for unambiguous optical detection of lunar impact plumes from earth-based observations (Ortiz et al. 2006). The era of artificial impact-induced transients started with the HiTen spacecraft launch in 1990. After orbiting the Earth for a time, it was redirected into lunar orbit and, on April 10, 1993, was crashed onto the lunar surface. Observers failed to detect visual images of the impact, but an infrared

observation from the Anglo-Australian Telescope did capture a rudimentary signal. The next recorded lunar impact was the SMART-1 probe in 2006. In this instance, the impact flash was captured in a few frames from an infrared detector at the Canada-France-Hawaii Telescope (Veillet & Fong 2007). The next artificial event will be impact of the LCROSS probe in 2009. The LCROSS (Lunar Crater Observation and Sensing Satellite) mission is to crash a 2000 kg mass onto the Moon's surface at 2.5 km/sec and ultimately create a large plume of lunar dust. A following spacecraft will acquire visual and infrared data on the impact in great detail. The objective of this article is to develop a quantitative model of the impact flash portion of this event where a significant amount of heat and light is emitted in a short burst.

Physical processes involving hypervelocity impacts are very complex and currently accepted mechanisms governing the process are considered in some detail in the monograph by Melosh 1989. The first indication of an impact is the vapor plume consisting of the vaporized impactor along with target material. Following the rapidly propagating vapor plume is the so-called "excavation flow" consisting of stress transients in the crust followed by the release of dust and other material in a large "ejecta curtain." These three sequential events are predictable (in theory, but not easily implemented) using the equations of gas dynamics; the equations of elastic-plastic deformation and flow; and finally by many-particle methods using the equations of ballistics.

The vapor plume (or impact flash) is probably most amenable to theoretical modeling as the equations of gas dynamics along with the associated state equations are reasonably

well known. In a terrestrial environment (where the molecular mean free path is measured in fractions of microns) the flare is followed by a detonation wave with a strong shock wave. Taylor 1950 showed how special solutions to the Euler equations for a polytropic gas can be used to predict the speed and strength of such a blast wave. On an airless body such as an asteroid or the Moon (where the mean free path is about 10 orders-of-magnitude greater than Earth) there is no precursor shock wave since high gradient flows are severely damped in rarefied flows. In a lunar impact only a flash and some thermal radiation will be emitted and can be detected for a short time in either visual or infrared wavelengths.

Particular solutions for the free expansion of a gas into a vacuum exist in the literature. Melosh 1989 considers a simple subset of these solutions using similarity arguments and a more detailed analysis may be found in Zel'dovich & Raizer 1966. In a general study of boundary value problems for compressible flow, Keller 1956 solves the equation for the free expansion of a gas into a vacuum. The analytical solution is unfortunately given in parametric form and involves higher transcendental functions, but is extremely useful in this application. Molmud 1960 solves the gas dynamic equations for vacuum expansion using a numerical procedure. In both cases, the initial conditions are somewhat restricted. In previous work only selected portions of the impact event are considered. In this article Keller's analytical solution is adopted to the problem and the flash event is predicted using only the kinetic energy of the impactor as an initial condition.

A key parameter set relating to the model is the initial state of the flare. These are initial values of pressure, density, temperature, and radius. They are estimated by making assumptions regarding the conversion of the initial kinetic energy of the impactor into heat energy. Thus, the initial condition is a small region of concentrated heat energy that dissipates and is quickly converted to wave kinetic energy as it expands into the lunar environment during which the sum of heat and kinetic energy is conserved. Using blackbody-type emission spectra at each radial position and time, the total integrated emission is computed by methods developed in protoplanetary nebula theory to predict the observed spectral broadening in such disks (Pringle 1981). Although this is a commonly used method in astrophysics, there is some evidence from scale-model testing on simulated targets that impact-induced radiation may be influenced by discrete spectral components (Ernst et al. 2006). However, wide band emission will be considered here pending detailed data from actual impacts that are not yet available. The total radiation measures the time-dependent emitted power that is the primary measurable output from the impact flare.

The gas dynamic solution

The Euler equations of motion for the spherically symmetric expansion of a polytropic gas are:

$$\frac{\partial \rho}{\partial t} + \frac{\partial(\rho u)}{\partial r} + \frac{2\rho u}{r} = 0$$
$$\frac{\partial \rho}{\partial t} + \frac{\partial(\rho u^2 + p)}{\partial r} + \frac{2\rho u^2}{r} = 0$$
$$p = k\rho^{\gamma}$$

These non linear equations for density, pressure and radial velocity possess few analytical solutions. Keller 1956 used a Lagrangian approach and his solution for

expansion into a vacuum is expressed in parametric form:

$$
\begin{aligned}
p &= p_0 j^{-3\gamma}\left(1-\left(\tfrac{r/r_0}{j/j_0}\right)^2\right)^{\gamma/(\gamma-1)} \\
\rho &= \rho_0 j^{-3}\left(1-\left(\tfrac{r/r_0}{j/j_0}\right)^2\right)^{1/(\gamma-1)} \\
T &= T_0 j^{-3(\gamma-1)}\left(1-\left(\tfrac{r/r_0}{j/j_0}\right)^2\right) \\
t &= t_0\sqrt{\tfrac{3}{\gamma}}\,\tfrac{\gamma-1}{3\gamma-1}e^{i\pi/2}\left\{ j^{(3\gamma-1)/2}\,{}_2F_1\left(\tfrac{3\gamma-1}{6\gamma-6},\tfrac{1}{2},\tfrac{9\gamma-7}{6\gamma-6},(j/j_0)^{3(\gamma-1)}\right) - j_0^{(3\gamma-1)/2}\,{}_2F_1\left(\tfrac{3\gamma-1}{6\gamma-6},\tfrac{1}{2},\tfrac{9\gamma-7}{6\gamma-6},1\right)\right\}
\end{aligned}
\tag{1}
$$

Equation (1) predicts the wave motion as j increases while j itself is a monotonically increasing inverse function of t as depicted in the last equation by hypergeometric functions. Its exact and asymptotic forms (where it reverts to a simple linear function) are described in the Appendix. The dependent variables p,ρ,T retain power-law-mediated parabolic forms in terms of j and $j = j_0$ represents the initial instant when the flare's characteristic radius is r_0. Two constraints are that the internal heat energy at $j = j_0$ (t = 0) is $\int_0^{r_0} p/(\gamma+1)2\pi r^2 dr$ and is related to the impactor kinetic energy and p_0, ρ_0, and T_0 are connected by the perfect gas law. These conditions relate two of the four initial parameters (p_0, ρ_0, T_0 and r_0). A length scale may be taken as the radius of the impactor and T_0 is retained as an open parameter. Velocity and time scales set by the initial conditions are $a_0 = \sqrt{p_0/\rho_0}$ and $t_0 = r_0/a_0$ respectively. The only remaining quantity is the specific heat ratio that, as will be shown, is the only factor governing the decay rate of the photometric signal.

A physically meaningful quantity is the speed of the expanding wave front which is computed from $u = r_0\, dj/dt$ where the time derivative of j is obtained from the inverse

relation t = t(j) given in the last of eq (1). The asymptotic value as $t, j \to \infty$ is $u = 2a_0\sqrt{\gamma/3}/(\gamma-1)$. This is slightly less than the maximum velocity for a self similar solution $2a_0\sqrt{\gamma}/(\gamma-1)$ as given by Zel'dovich & Raizer 1966 using a different distribution of the initial pressure and density. Wave front velocities and physical time are illustrated in Figure 1 as functions of the parameter j for specific heat ratios of monatomic (γ = 5/3) and diatomic (γ = 7/5) ideal gases. The asymptotic wave front speeds (horizontal lines in Figure 1a) are independent of j (or t) while the evolving solution approaches these limiting values from below as j increases. Smaller values of the specific heat ratio imply a slower approach to self similarity so that self similarity may not actually be satisfied for some impact flare events. The physical time is shown in Figure 1(b) for the same two values of γ. In each case the exact curve (expressible in terms of higher transcendental functions) reverts to a simple linear form whose slope is directly proportional to the wave speed. With a polytropic gas approximation there is no expectation that the ratio of specific heats be restricted to the specific values used above and is considered a free parameter in determining the appropriate power law for the emitted luminance.

Heat and light emission from the flare

Equation (1) is a parametric representation of the flare event. Assuming blackbody thermal emission at radial temperature T(r), the spectral distribution of thermal energy at any instant can be expressed as the spectral radiance in terms of a non dimensional Planck function:

$$B(j,\Lambda,\eta;\gamma)=2\Lambda^{-5}\left(\mathrm{Exp}\left(\frac{j^{3(\gamma-1)}}{\Lambda(1-\eta^2)}\right)-1\right)^{-1}$$

The normalization factor is $k^5T_0^5/c^3h^4$ W/m^3 in terms of Planck constant (k), speed of light (c), and Boltzmann constant (h). The wavelength and spatial non-dimensional parameters are: $\Lambda = kT_0\lambda / ch$ and $\eta = r / r_j = r / jr_0$ where λ is the physical wavelength and r_j is the instantaneous radius of the wave front. The opacity of the hemispherical flare is considered low enough so that thermal emission is restricted to the trace of the flare on the lunar surface. The total emitted spectrum from each concentric ring at temperature T is computed following the same procedure used by Pringle 1981 in his studies of spectral emission by protoplanetary disks. In this case the total spectral radiance at each instant is computed according to the integral

$$G(j,\Lambda;\gamma) = \frac{j^2 r_0^2 k^5 T_0^5}{c^3 h^4} \int_{\eta=0}^{1} \mathrm{B}(\mathrm{j},\Lambda,\eta;\gamma) 2\pi\eta \mathrm{d}\eta \text{ W/m/sr} \tag{2}$$

which must be integrated numerically for each choice of γ. Finally, the total time dependent radiant intensity is the integral of G over the entire wavelength range and is computed from

$$L(j;\gamma) = \frac{ch}{kT_0} \int_{\Lambda=0}^{\infty} G(j,\Lambda;\gamma) d\Lambda \text{ W/sr} \tag{3}$$

This quantity depends only on time (through the parameter j) and the specific heat ratio γ. It predicts the time dependent radiant intensity; a measurable quantity relating to the flare event. The intensity computed from eq (3) is found to obey a simple power law $L(t) \sim t^p$ where p depends only on the specific heat ratio. Application of these formulas is illustrated in the following sections by comparison with an impact experiment in a gun tunnel and with predictions of the LCROSS lunar vapor plume.

Comparison with a Simulated Impact Flash

Impact experiments to simulate vapor plumes on extra terrestrial bodies are described in a series of presentations (Ernst & Schultz 2002, 2003, 2007; Ernst et al. 2006) using impactors of 0.635 cm diameter Pyrex or copper spheres. Data from these experiments include intensity time histories from the flare. They are characterized by a rapid rise in photometric intensity followed by a slower decay over a total time scale of about 1000 μs. In Ernst & Schultz 2003 the decay is shown to obey a simple algebraic power law that is consistent with eq (3) with a value of the exponent p ranging from -0.3 to -1.3 with a variety of targets. The decay was also found to be independent of the impact velocity, a measure of the initial kinetic energy. Analysis of eq (3) shows that the specific heat ratio ranges from 1.19 to 1.27 for these exponents.

Measured decay curves (Ernst et al. 2006) to an arbitrary vertical scale are indicated in Figure 2 by solid symbols for two of the target materials. The targets are high porosity powdered and solid pumice in fig 2(a) and (b). The measured signal from each event was found to consist of a rapid rise and a subsequent power law decay rate of -0.6 and -1.01 for the powdered and solid pumice. These rates are fit to the model described above and correspond to effective specific heat ratios of 1.216 and 1.250 respectively. Once the decay rate is determined, the only remaining fit-parameter is the characteristic time t_0. It value is determined by expanding or contracting the time scale appropriately. The values are found to be 20 and 40 μs respectively. These analytical decay curves are shown in the figure as solid lines. The overall fit to the measured signal is quite good considering the assumptions made in the derivation of the decay law.

The LCROSS flash event

The solution depends on three conditions at t = 0 which is the instant when both impactor and target material are vaporized into a gas cloud. These are the radius of the cloud, the pressure, and the density at the cloud center (r_0, p_0, ρ_0). The LCROSS projectile imparts a directed kinetic energy of 6250 MJ. (For comparison, 1 lb of high explosive has an energy content of about 2.2 MJ so the impact is equivalent to approximately 3000 lb of high explosive.) The fraction of this kinetic energy converted into internal heat energy (the "efficiency factor") is taken as 0.2% of the impact kinetic energy following Ortiz et al. 2006. Thus, the internal energy at t = 0 is 12.5 MJ which, following its definition, implies a relationship between p_0 and r_0. The initial radius of the cloud is taken as that of the LCROSS impactor of 1.1 m so the initial pressure is 6.56 MPa. Furthermore, the initial temperature is estimated as about 2000 K. Assuming certain thermodynamic and chemical properties of the vaporized gas such as its specific heat ratio (γ =1.21) and atomic weight (μ ~ 50 g/mole corresponding to a combination of the aluminum impactor and the lunar regolith) the value of ρ_0 from the perfect gas law is 20 kg/m^3. These values incorporated into eq (1) fully define the evolution of the vapor plume.

Using the stated parameters, the velocity and time scales for the impact are a_0 = 577 m/s and t_0 = 1.9 ms. The speed and location of the advancing wave front are illustrated in figure 3 in physical units. The limiting wave speed $u_1 = 2a_0\sqrt{\gamma/3}/(\gamma-1)$ is 3400 m/s. The average self similar speed u_∞ of the vapor plume assuming that all the heat energy is converted to kinetic energy is computed from $1/2Mu_\infty^2 = E_{\text{int@}t=0}$ and is 1586 m/s. The relation between these speeds is $u_1 = 2.18u_\infty$ which is close to Zel'dovich & Raizer's

value of $u_1 = 1.92u_\infty$ for a different value of γ (1.33). In figure 3(a) the plume's time dependent wave velocity approaches its limiting value asymptotically from below. This slow approach is because the wave speed reaches it final value only at the rate of $1\text{-}j^{-0.63}$. This specific heat mediated approach to similarity is also illustrated in figure 1(a) using other values of γ. The wave front evolution from Figure 3(b) asymptotically approaches a linear law that indicates a similarity solution.

The broad band optical/thermal spectrum at each instant is synthesized from an integral of blackbody spectra at each radial position following eq (2). A sequence of such signals is shown in figure 4 at seven times during the evolution of the flash. The spectra are reminiscent of classical blackbodies but the spectrum is broader and biased toward reddening. Such spectral broadening is not as extensive as that observed in protoplanetary disks and in this case the spectral maxima are shifted towards the infrared by about 17% relative to the blackbody at that temperature.

The luminosity curve is now computed directly from eq (3) and is depicted in figure 5. In the main logarithmic log scale it decays as t^{-058}. A power law with the same exponent is shown by the dashed line. Starting from a radiant intensity of 190 KW per solid angle, it drops by an order of magnitude in about 100 ms while the spectral peak (fig 4) moves towards the infrared. The inset graph shows the radiant flux as perceived on Earth converted into the magnitude scale. The equivalent magnitude at t ~ 0 is 10.9 (relative to the Sun at -26.7) and decays according to the power law prescription. This level of brightness is accessible by larger telescopes since a 4-m class telescope can collect data up to magnitude 20.

Conclusions

Vapor plume evolution due to transient impacts can be characterized by a few parameters. From measured luminosity time histories two key parameters emerge: the time scale t_0 and the equivalent specific heat ratio. If the wave speed can be constrained by measurement, the characteristic velocity a_0 along with the initial scale $r_0 = a_0\, t_0$ can be computed. These parameters can be used to effectively compare different events.

This analysis is restricted to the evolution of the vapor plume. Details concerning the conversion of directed kinetic energy into the short-duration vapor plume and the longer time phenomena such as excavation flows and dust curtains require considerably more detailed analysis.

Appendix

The parametric representation for the time variable is give by Keller 1956 as the solution of a nonlinear first order ordinary differential equation for j(t)

$$\left(\tfrac{dj}{dt}\right)^2 = C_1(1 - j^{3(\gamma-1)})$$

where $\gamma > 1$ assures positive exponent. The inverse solution for t as a function of j is given by the improper integral

$$t = C_1 \int \frac{1}{\sqrt{1 - j^{-3(\gamma-1)}}} dj$$

and can be expressed in terms of the Gaussian hypergeometric function (Abramowitz & Stegun 1964). The final formula satisfying the initial condition is

$$t = t_0 \sqrt{\tfrac{3}{\gamma}}\, \tfrac{\gamma-1}{3\gamma-1} e^{i\pi/2} \left\{ j^{(3\gamma-1)/2}\, {}_2F_1\left(\tfrac{3\gamma-1}{6\gamma-6}, \tfrac{1}{2}, \tfrac{9\gamma-7}{6\gamma-6}, (j/j_0)^{3(\gamma-1)}\right) - j_0^{(3\gamma-1)/2}\, {}_2F_1\left(\tfrac{3\gamma-1}{6\gamma-6}, \tfrac{1}{2}, \tfrac{9\gamma-7}{6\gamma-6}, 1\right) \right\} \quad \text{(A1)}$$

Here $\gamma > 1$ and ${}_2F_1(a,b,c,z)$ is the hypergeometric function of the three indicated parameters and its argument z. These functions are not easy to work with are easily accessible using modern symbolic algebra software. Special values of the parameters vastly simplify this equation. For example, using a monatomic gas when $\gamma = 5/3$, it reduces to algebraic formula as illustrated below.

When $j = j_0$ the expression vanishes since t = 0 and when j becomes large it approaches self similarity with t linearly related to j. This is shown by using asymptotic formulas from Erdelyi 1953. For large values of its argument z, the first term in braces in eq (A1) becomes

$$j^{\frac{3\gamma-1}{2}}\,{}_2F_1(a,b,c,z) \approx j^{\frac{3\gamma-1}{2}}\left(\lambda_1 z^{-a} + \lambda_2 z^{-b}\right) =$$
$$\lambda_1 j^{\frac{3\gamma-1}{2}}\left(j^{3(\gamma-1)}\right)^{-\frac{3\gamma-1}{6\gamma-6}} + \lambda_2 j^{\frac{3\gamma-1}{2}}\left(j^{3(\gamma-1)}\right)^{-\frac{1}{2}} =$$
$$\lambda_1 + \lambda_2 j$$

where λ_1 and λ_2 are (complex) constants. This expression is a simple linear form that when combined with eq (A1) becomes the similarity solution. The second proportionality constant is directly related to the wave speed, but it is much easier to compute this value numerically from the exact representation.

References

Abramowitz, M. & Stegun, I. A.(Eds.) 1964. Handbook of Mathematical Functions. National Bureau of Standards, Washington, DC. AMS Series No 55. p 555.

Cameron, W. S. 1972. Comparative analysis of observations of lunar transient phenomena. Icarus 16,339-387

Cameron, W. S. 1975. Manifestations and possible sources of lunar transient phenomena. Earth, Moon, and Planets. 14,187-199.

Erdelyi, E. (Ed.) 1953. Higher Transcendental Functions Vol 1. McGraw Hill, New York. p 76.

Ernst, C. M. & Schultz, P. H. 2002. Effect of Velocity and Angle on Light Intensity Generated by Hypervelocity Impacts. Lunar Planet. Sci. Conf. XXXIII, abstract #1782.

Ernst, C. M. & Schultz, P. H. 2003. Effect of Initial Conditions on Impact Flash Decay. Lunar Planet. Sci. Conf. XXXIV, abstract #2020.

Ernst, C. M. & Schultz, P. H. 2007. Temporal and Spatial Resolution of the Early-time Impact Flash: Implications for Light Source Distribution. Lunar Planet. Sci. Conf. XXXVIII, abstract #2353.

Ernst, C. M., Schultz, P. H. & A' Hearn, M. F. 2006. Photometric Evolution of the Deep Impact Flash. Lunar Planet. Sci. Conf. XXXVII, abstract #2192.

Hughes, D. 1980. Transient lunar phenomena. Nature 285,438

Keller, J. B. 1956. Spherical, cylindrical and one-dimensional gas flows. Quart. J. Appl. Math. 14,171–184.

Melosh, H. J. 1989. Impact Cratering, a Geologic Process. Oxford University Press, New York.

Molmud, P. 1960. Expansion of a rarefied gas cloud into a vacuum. Phys. Fluids. 3, 362-366.

Ortiz, J., Aceituno, F., Quesada, J., & Aceituno, J. 2006. Detection of sporadic impact flashes on the Moon: implications for the luminous efficiency of hypervelocity impacts and derived terrestrial impact rates. Icarus 184,319-326.

Pringle, J. E. 1981. Accretion disks in Astrophysics. Ann. Rev. Astron. Astrophys. 19,137-162.

Taylor, G. 1950. The formation of a blast wave by a very intense explosion: I. Theoretical discussion. Proc. Roy. Soc. A201,159–174.

Veillet, C. & Fong, B. 2007. Smart-1 impact observations at the Canada-France-Hawaii Telescope. Lunar Planet. Sci. Conf. XXXVIII, abstract #1520.

Zel'dovich Ya. B. & Raizer, Yu. P. 1966. Physics of Shock Waves and High Temperature Hydrodynamic Phenomena. (Eds. W. D. Hayes & R. F. Probstein). Academic Press, New York.

Figure Legends

Figure 1.Wave front speeds (a) and physical time (b) as functions of the parameter j. Both quantities are normalized by the velocity and time scales set by the initial distribution. The asymptotic velocity ratios are 2.24 ($\gamma = 5/3$) and 3.42 ($\gamma = 7/5$)

Figure 2. Radiant flux (arbitrary scale) for experimental impact (solid symbols) compared with gas dynamic based flare theory (solid line). The power law decay rate is determined solely by the ratio of the specific heats and the reference time is computed by scaling of the time axis to the experimental data. The target material is (a) powdered pumice; (b) solid pumice.

Figure 3. Time evolution of the LCROSS impact flare event indicating wave front velocity (a) and location (b). The wave front closely approximates the self similar variable r/t = 3400 m/s (light horizontal line in (a)); but approaches this limiting speed only asymptotically during the timeline considered.

Figure 4. Instantaneous spectral radiant intensity during the simulated LCROSS impact. Values of the time(ms) are noted on the figure for each spectrum. The maximum temperature (K) and wave length (μm) of the spectral peak for each indicated time are: (08, 1988, 1.73), (1.4, 999, 3.38), (2.22, 725, 4.68), (3.73, 500, 6.76) (5.88, 363, 9.35), (10.7, 240, 14.2), and (17.3, 172, 19.8) respectively.

Figure 5. Luminous flux from the impact showing evolution into a power law decay. The inset shows the same data to a linear scale of magnitude vs. time as would be observed by an earth-based telescope.

Fig 1

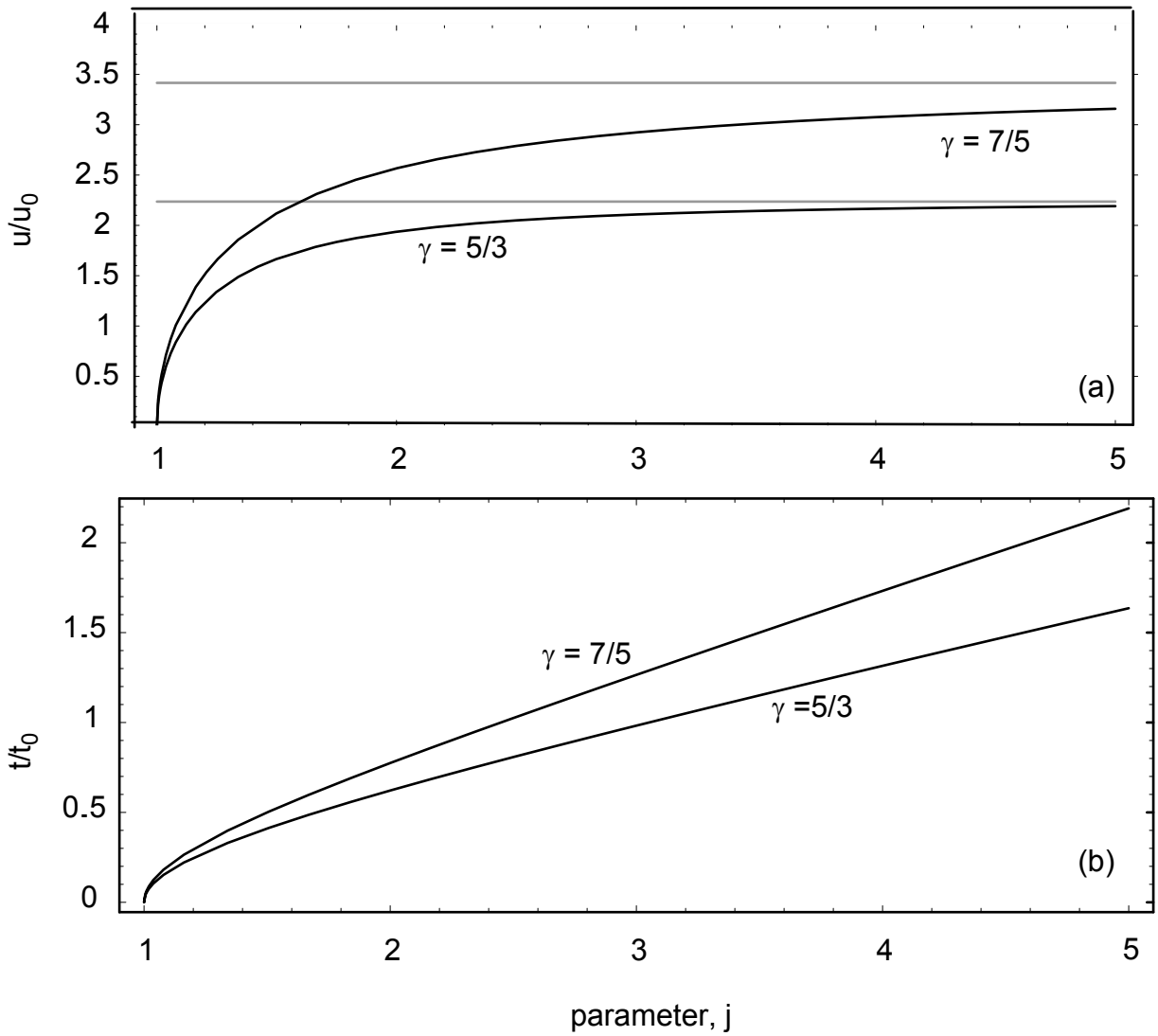
4
3.5
3
2.5
2
1.5
1
0.5
u/u0
γ = 7/5
γ = 5/3
(a)
1
2
3
4
5
2
1.5
1
0.5
0
t/t0
γ = 7/5
γ =5/3
(b)
1
2
3
4
5
parameter, j

Fig 2

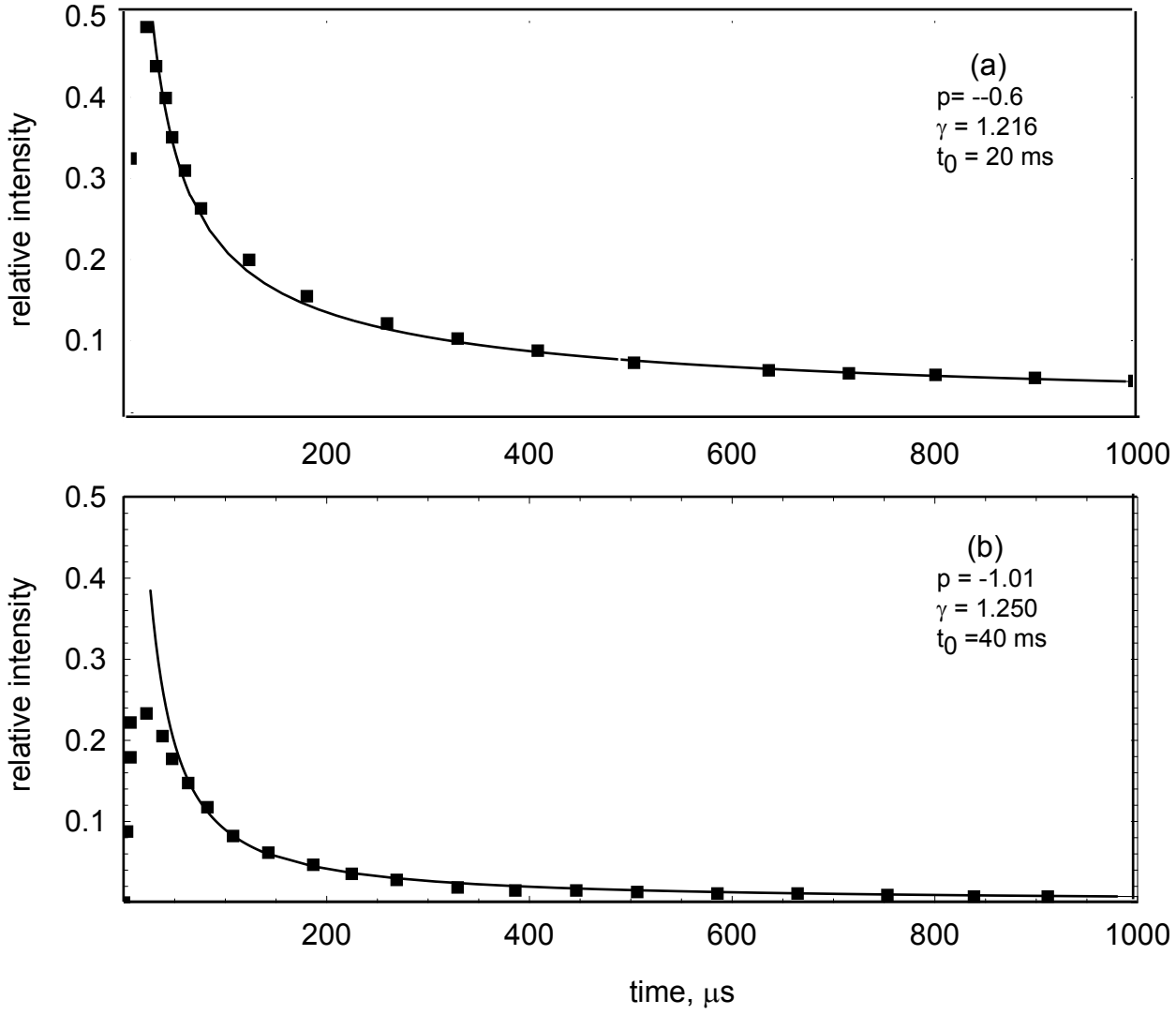
0.5
0.4
0.3
0.2
0.1
relative intensity
(a)
p= --0.6
γ = 1.216
t0 = 20 ms
200
400
600
800
1000
0.5
0.4
0.3
0.2
0.1
relative intensity
(b)
p = -1.01
γ = 1.250
t0 =40 ms
200
400
600
800
1000
time, μs

Fig 3

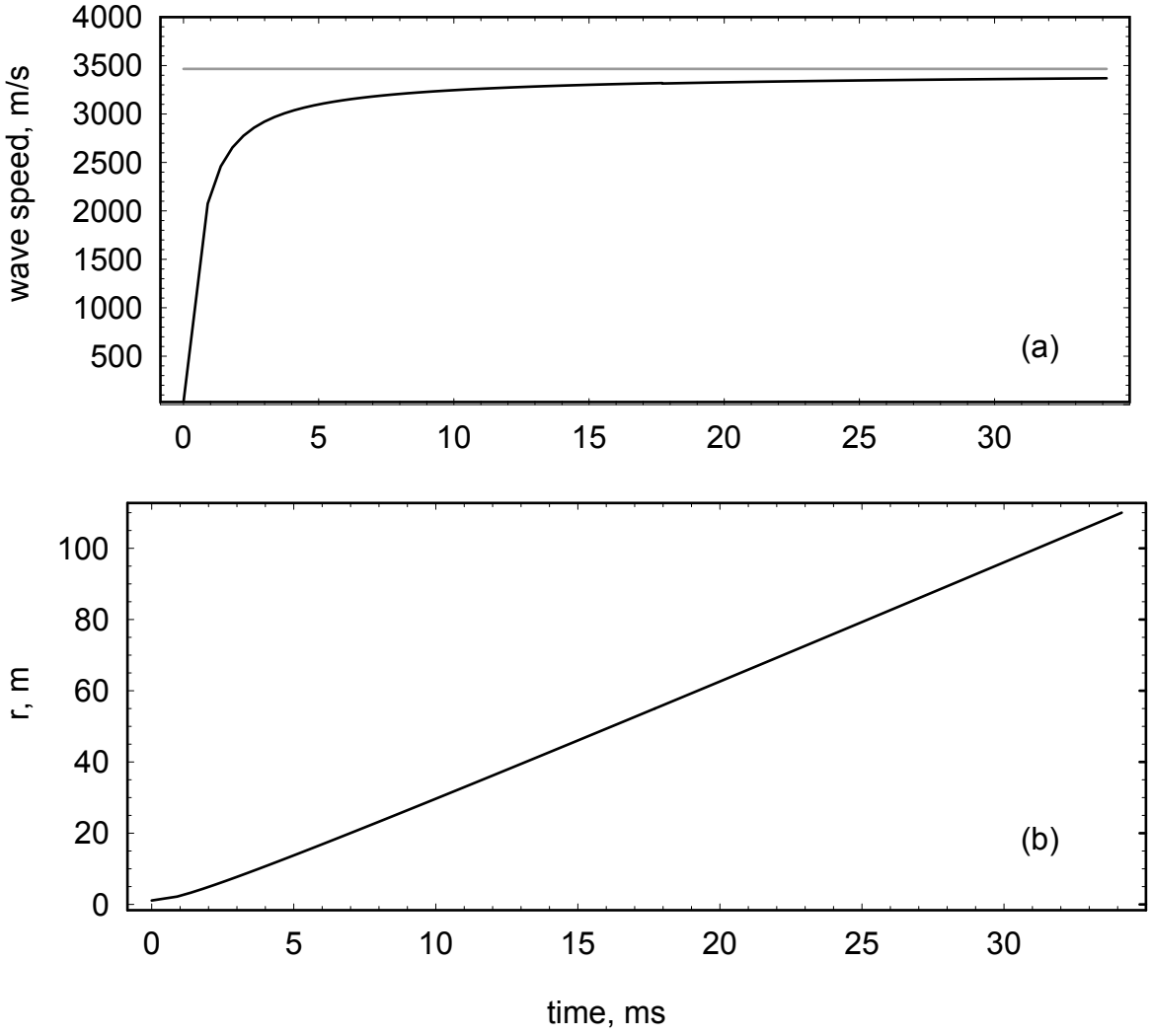
4000
3500
3000
2500
2000
1500
1000
500
wave speed, m/s
(a)
0
5
10
15
20
25
30
100
80
60
40
20
0
r, m
(b)
0
5
10
15
20
25
30
time, ms

Fig 4

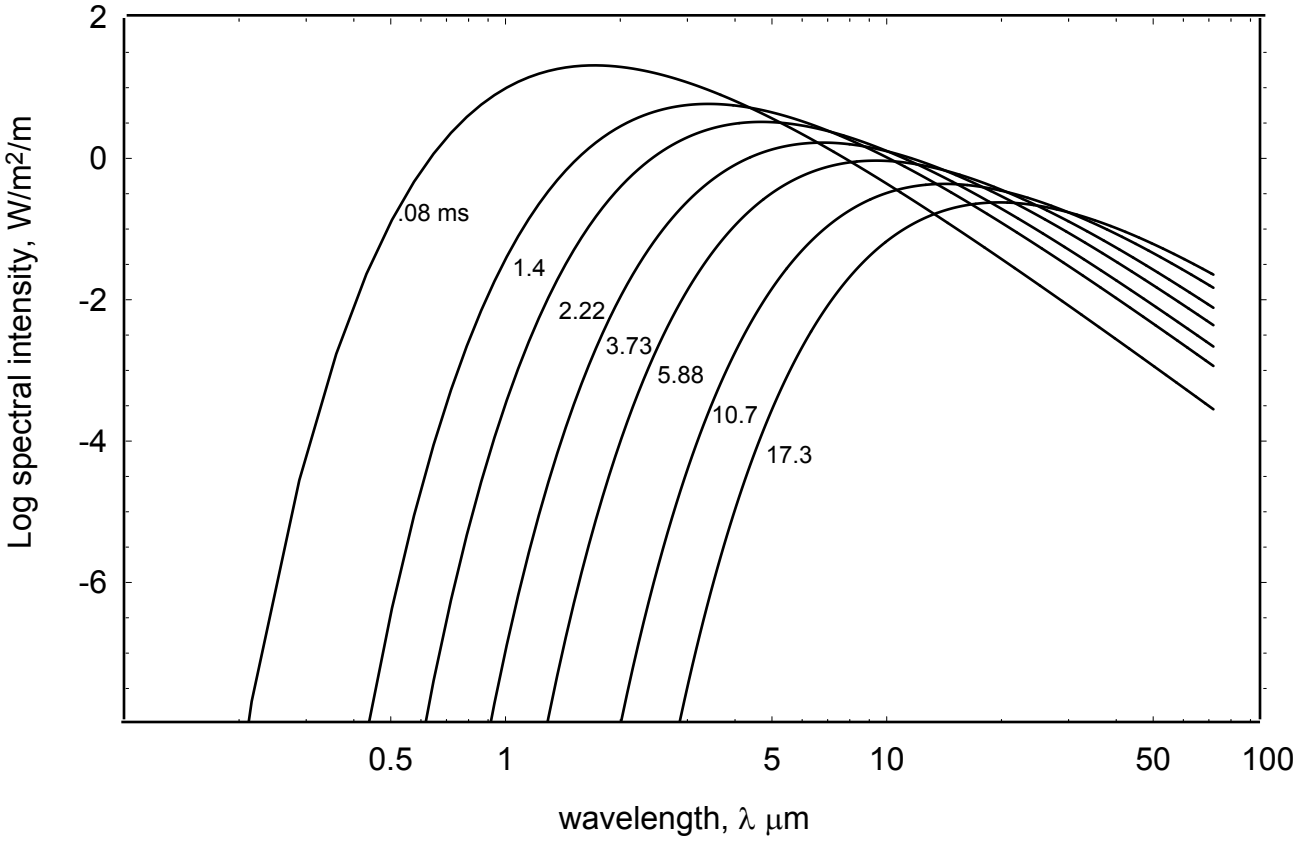
2
0
-2
-4
-6
Log spectral intensity, W/m2/m
.08 ms
1.4
2.22
3.73
5.88
10.7
17.3
0.5
1
5
10
50
100
wavelength, λ μm

Fig 5

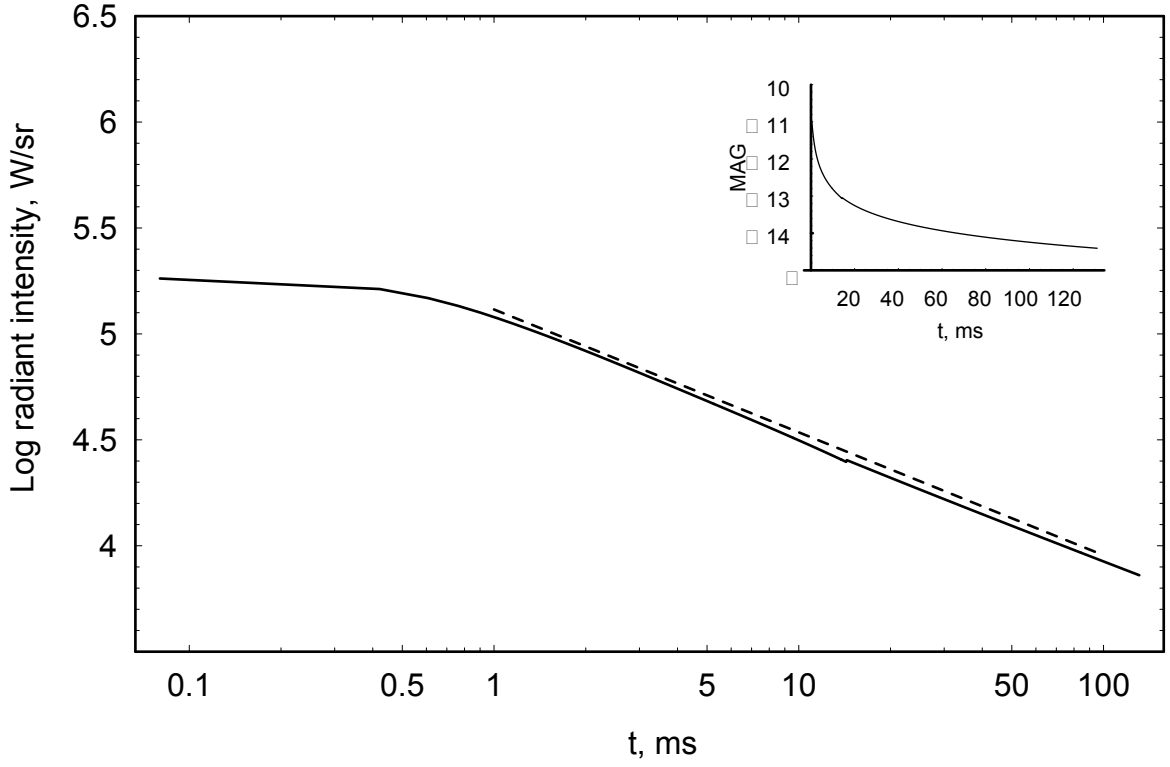
6.5
6
5.5
5
4.5
4
Log radiant intensity, W/sr
0.1
0.5
1
5
10
50
100
t, ms
10
11
12
13
14
MAG
20
40
60
80
100
120
t, ms